Sensitivity of polarized neutron-polarized ^{3}He scattering to the excited level structure of ^{4}He

C. D. Keith, C. R. Gould, and D. G. Haase
North Carolina State University, Raleigh, North Carolina 27695
and Triangle Universities Nuclear Laboratory, Durham, North Carolina 27708

N. R. Roberson and W. Tornow
Duke University, Durham, North Carolina 27708
and Triangle Universities Nuclear Laboratory, Durham, North Carolina 27708

G. M. Hale
Los Alamos National Laboratory, Los Alamos, New Mexico 87545

H. M. Hofmann
Institut für Theoretische Physik III, Universität Erlangen-Nürnberg, Staudtstrasse 7, D-91058 Erlangen, Germany

H. Postma
University of Technology, P.O. Box 5046, 2600 GA Delft, The Netherlands
(Received 23 February 1994)

Calculations of polarized neutron-polarized ^{3}He scattering are presented for the transverse and longitudinal total cross-section differences $\Delta\sigma_T$ and $\Delta\sigma_L$ in the energy range $E_n = 0.1$ to 10 MeV. Predictions made from phase-shift analyses, R-matrix analysis, and a multichannel resonating group model calculation are compared. The predictions are in qualitative agreement and show that polarized neutron-polarized ^{3}He scattering is sensitive to the level structure of ^{4}He in the excitation energy range 20–30 MeV.

PACS number(s): 21.45.+v, 24.70.+s, 25.10.+s, 27.10.+h

I. INTRODUCTION

In the past two decades the four-nucleon system, particularly the α particle, has received a great deal of experimental and theoretical attention [1]. Of all nuclei, ^{4}He is the lightest system that possesses both bound and excited states. As such it represents a unique laboratory for understanding few-nucleon dynamics.

Exact four-body calculations of the ^{4}He ground state using realistic nucleon-nucleon potentials have already been performed with considerable success by the Bochum [2] and Groningen [3] groups. Efforts to extend these calculations to the continuum are currently underway [4] but are expected to be considerably more difficult. Whereas the ^{4}He ground state is an extremely symmetric and tightly bound system, the continuum states are surprisingly complex. A recent, comprehensive R-matrix analysis of four-nucleon scattering and reaction data finds evidence for as many as 15 resonant levels 20–30 MeV above the ^{4}He ground state [1,5]. None of the excited states are bound. That is, each of the above mentioned 15 states is unstable against break-up into the p-^{3}H, n-^{3}He, d-D, or three- or four-body channels. Additionally, P- and D-wave scattering play an important role in the structure of the ^{4}He continuum, and the degree of isospin mixing between the $T = 0$ and $T = 1$ states is not fully understood.

Polarization observables are essential for the unique determination of few-body scattering amplitudes. A polarized-target–polarized-beam experiment is being conducted at the Triangle Universities Nuclear Laboratory (TUNL) to measure the spin dependence of the total neutron cross section of ^{3}He. In preparation for the experiment, calculations of the spin-dependent total cross-section difference $\Delta\sigma$ have been performed based on the resonance structure of Ref. [5]. Calculations are presented for spin geometries in which the target and projectile spins are longitudinal ($\Delta\sigma_L$) and transverse ($\Delta\sigma_T$) to the beam momentum. Additionally, calculations have been made based on two partial-wave analyses of n-^{3}He scattering [6,7], as well as on a microscopic resonating group model (MCRGM) analysis of ^{4}He [8].

II. FORMALISM

The formalism for the scattering of polarized neutrons from a polarized or aligned target has been presented elsewhere [9,10]. In the former, the coupling of angular momenta is expressed in the "j-spin" representation, whereas in few-body systems the "channel-spin" representation is standard. The latter article is not consistent with the Madison convention [11] in its definition of statistical tensors describing the polarization state of the

beam and target. Also, [10] expresses cross sections in terms of the partial neutron width amplitudes γ_{ls} which are ill-suited for broad, overlapping levels such as those displayed in the ^{4}He nucleus. We present an exact formula for the total neutron cross section in terms of scattering matrix elements using the channel-spin representation. For the special case of spin-1/2 targets, the total cross section is expanded in terms of the integrated partial-wave cross sections, and methods of extracting information on specific partial waves are discussed.

To describe the polarization states of the beam and target, we use the statistical tensors, $t_{kq}(I_a)$ and $t_{KQ}(I_A)$, respectively, defined according to the Madison convention [11]

$$t_{KQ}(I) = \hat{I}\sum_{m}(-1)^{I-m}\rho_{mm'}(I)\langle IIm' - m|KQ\rangle. \quad (1)$$

Here I is the spin of the target (or neutron), $\hat{I} = \sqrt{2I+1}$, and $\rho_{mm'}(I)$ is the density matrix of magnetic substates. With this definition, t_{00} is equal to 1. This equation can be easily inverted to write the density matrix in terms of the statistical tensors

$$\rho_{mm'}(I) = \hat{I}\sum_{KQ}(-1)^{I-m}t_{KQ}(I)\langle IIm' - m|KQ\rangle. \quad (2)$$

Typically, a polarized target or beam is prepared such that there is an axis of cylindrical symmetry (the "spin axis"). If this axis is chosen as the z axis, then the spin tensors calculated in this coordinate system, $\tilde{t}_{KQ}$, are diagonal, and the only nonvanishing elements are those with $Q = 0$. Additionally, the $Q = 0$ components are real quantities. The spin tensors calculated in a different coordinate system (for example, one in which the z axis is along the beam direction) can be expressed in terms of the $\tilde{t}_{K0}$ by the rotation

$$\begin{aligned} t_{KQ}(I) &= \sqrt{\frac{4\pi}{2K+1}}Y_K^Q(\beta_I,\phi_I)\tilde{t}_{K0}(I) \\ &= C_{KQ}(\beta_I,\phi_I)\tilde{t}_{K0}(I), \end{aligned} \quad (3)$$

where β_I and ϕ_I are the polar and azimuthal angles that the spin axis makes in the new coordinate system and $Y_K^Q(\beta_I,\phi_I)$ is a normalized spherical harmonic [12]. This coordinate system is shown in Fig. 1.

The spin-dependent, elastic-scattering amplitude, with the z axis along the incident neutron beam direction $\vec{k}$, can be written as [13]

$$\begin{aligned} f_{\substack{m'_A m'_a \\ m_A m_a}}(\theta,\phi) = i\sqrt{\pi}\lambda \sum_{\substack{J,l,l' \\ s,s',m_s}} \hat{l}\langle I_A I_a m_A m_a|s\, m_s\rangle\langle ls0m_s|J\, m_s\rangle\langle I_A I_a m'_A m'_a|s' m_{s'}\rangle\langle l's'\, m_s - m_{s'},\, m_{s'}|J\, m_s\rangle \\ \times\left[\delta_{l'l}\delta_{s's} - S^J_{ls,l's'}\right]Y_{l'}^{m_s-m_{s'}}(\theta,\phi), \end{aligned} \quad (4)$$

where $\lambda = \hbar/\mu v$ (μ is the reduced mass and v is the center-of-mass velocity), and l and l' are the incoming and outgoing orbital angular momenta. Likewise, s and s' are the incoming and outgoing channel-spin momenta, and m_s, etc., are their z components. $S^J_{ls,l's'}$ is the scattering matrix element for transitions from the initial neutron channel (Jls) to the final channel ($Jl's'$). The angular momentum coupling order is

$$\begin{aligned} \vec{J} &= \vec{l} + (\vec{I}_A + \vec{I}_a) \\ &= \vec{l} + \vec{s}. \end{aligned} \quad (5)$$

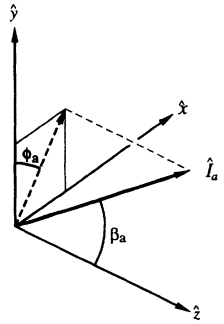

FIG. 1. The coordinate system defined according to the Madison convention [11]. Here $\hat{z}$ is along the incident beam direction $\hat{k}$. The $\hat{y}$ axis is along the $\hat{k}\times\hat{k}'$ direction ($\hat{k}'$ is the direction of the scattered beam), and the $\hat{x}$ axis is defined so as to make a right-handed coordinate system. The "spin axis" $\hat{I}_a$ is defined to be that axis in which the polarization tensor $\tilde{t}_{kq}$ is diagonal. A similiar coordinate system is defined for the target spin axis $\hat{I}_A$.

The total cross section $\sigma_{\rm tot}$ can be expressed in terms of the forward elastic-scattering amplitude via the generalized spin-dependent optical theorem [14]

$$\sigma_{\rm tot} = {\rm Im}\left\{4\pi\lambda\sum_{\substack{m_A m_a \\ m'_A m'_a}}\rho_{m_A m'_A}\rho_{m_a m'_a}f_{\substack{m'_A m'_a \\ m_A m_a}}(0^\circ)\right\}, \quad (6)$$

where $\rho_{m_A m'_A}$ and $\rho_{m_a m'_a}$ are the density matrices for the target and beam, respectively, and Im indicates the imaginary part of the complex argument. Substitution of Eqs. (2) and (4) into Eq. (6) yields the following formula for the total neutron cross section:

$$\sigma_{\rm tot} = {\rm Re}\Bigg\{ 2\pi\lambda^2 \sum_{\substack{Jll' \\ ss'}} \sum_{\substack{KQ \\ kq}} \sum_{\substack{m_A m_a \\ m'_A m'_a}} (-1)^{I_A+I_a-m_A-m_a} \hat{l}\hat{l}' \hat{I}_A^{-1} \hat{I}_a^{-1} \langle I_A I_A m'_A - m_A | KQ\rangle \langle I_a I_a m'_a - m_a | kq\rangle \langle I_A I_a m_A m_a | s m_s\rangle$$

$$\times \langle ls0m_s | Jm_s\rangle \langle l's' m_s - m_{s'} m_{s'} | Jm_s\rangle \langle I_A I_a m'_A m'_a | s' m_{s'}\rangle t_{KQ}(I_A) t_{kq}(I_a) \left[\delta_{l'l}\delta_{s's} - S^J_{lsl's'}\right] \Bigg\}. \tag{7}$$

Equation (7) can be reduced to a slightly less cumbersome form by the use of standard angular momentum coupling relations [12]. The final form contains no summation over the magnetic quantum numbers m_α. We write the total cross section as an expansion in terms of the polarization tensors calculated in the "spin-axis" coordinate system,

$$\sigma_{\rm tot} = \sum_{kK} \sigma_{kK} \tilde{t}_{K0}(I_A) \tilde{t}_{k0}(I_a), \tag{8}$$

where

$$\sigma_{kK} = {\rm Re}\Bigg\{ 2\pi\lambda^2 \sum_{\substack{Jll' \\ ss'}} \sum_{q} \frac{2J+1}{(2I_a+1)(2I_A+1)} F_q(Jlsl's') \left[\delta_{ll'}\delta_{ss'} - S^J_{lsl's'}\right] C^*_{Kq}(\beta_A,\phi_A) C_{kq}(\beta_a,\phi_a) \Bigg\} \tag{9}$$

and

$$F_q(Jlsl's') = \sum_{\Lambda} (-1)^K (-1)^{(J-s')} \hat{\Lambda} \hat{I}_a \hat{I}_A \hat{l}\hat{l}' \hat{s}\hat{s}' \hat{k} \langle \Lambda k 0q | Kq\rangle \langle l'l00 | \Lambda 0\rangle W(s'sl'l;\Lambda J) \begin{Bmatrix} I_a & s & I_A \\ I_a & s' & I_A \\ k & \Lambda & K \end{Bmatrix}. \tag{10}$$

Here $W(s'sl'l;\Lambda J)$ is a Racah angular momentum coupling coefficient, and the expression in the curly brackets is a 9-j symbol [12]. $\vec{\Lambda}$ is the orbital angular momentum transfer $\vec{l}' - \vec{l}$.

III. PARTIAL-WAVE DECOMPOSITION FOR SPIN-1/2 PARTICLES

For the specific case in which both target and projectile are spin-1/2 particles, the expression for the total cross section can be greatly simplified. In particular, the expansion in Eq. (7) contains only four terms

$$\sigma_{\rm tot} = \sigma_{00} + \sigma_{01}\tilde{t}_{10}(I_A) + \sigma_{10}\tilde{t}_{10}(I_a) + \sigma_{11}\tilde{t}_{10}(I_A)\tilde{t}_{10}(I_a). \tag{11}$$

The middle two terms are parity-violating contributions to the total cross section and may be ignored here. σ_{00} is simply the unpolarized total cross section (henceforth written as σ_0). σ_{11} is the contribution to the cross section arising from spin-spin interactions and is often referred to as the *spin-spin* cross section. Since the polarization tensor for the beam (or target) $\tilde{t}_{10}$ changes sign whenever the spin is reversed, the spin-spin cross section can be determined from the total cross-section difference $\Delta\sigma$:

$$\Delta\sigma = \frac{\sigma_{\rm tot}(++) - \sigma_{\rm tot}(+-)}{\tilde{t}_{10}(I_A)\tilde{t}_{10}(I_a)} = \frac{2\sigma_{11}}{\tilde{t}_{10}(I_A)\tilde{t}_{10}(I_a)}. \tag{12}$$

The (+) and (−) signs are used to indicate the relative orientation of the beam and target spins with respect to their respective spin axes. Experimentally, $\Delta\sigma$ may be determined from the "spin-spin asymmetry" $\varepsilon_{\rm SS}$. To measure $\varepsilon_{\rm SS}$, polarized neutrons are transmitted through a polarized target. The neutron spin (or target spin) is periodically reversed and the corresponding 0° yields are compared according to

$$\varepsilon_{\rm SS} = \frac{N(++) - N(+-)}{N(++) + N(+-)} = -\tanh\left[\frac{1}{2}\Delta\sigma\,\tau_A\,\tilde{t}_a\,\tilde{t}_A\right]. \tag{13}$$

Here $N(++)$ is the neutron yield at 0°, and $N(+-)$ is the same yield after one of the spins has been reversed. τ_A is the thickness of the polarized target in units of atoms per barn.

Typically, such experiments are performed with the beam and target spin axes parallel. The most common spin geometries are those in which the spins are parallel (longitudinal) or perpendicular (transverse) to the incident beam direction. The corresponding $\Delta\sigma$'s can be pictorially represented in the following manner:

$$\Delta\sigma_L = \sigma_{\rm tot}(\vec{\rightarrow}) - \sigma_{\rm tot}(\vec{\leftarrow}), \tag{14}$$

$$\Delta\sigma_T = \sigma_{\rm tot}(\uparrow\uparrow) - \sigma_{\rm tot}(\uparrow\downarrow), \tag{15}$$

where it is understood that $\Delta\sigma_L$ and $\Delta\sigma_T$ are normalized to unit beam and target polarizations.

Both σ_0 and σ_{11} can be decomposed into partial waves as follows. The cross section corresponding to the $(Jlsl's')$ S-matrix element is

$$\sigma(Jlsl's') = \mathrm{Re}\left\{ 2\pi\lambda^2 \frac{2J+1}{(2I_a+1)(2I_A+1)} \left[\delta_{ll'}\delta_{ss'} - S^J_{lsl's'}\right] \right\}. \tag{16}$$

In general, these "partial-wave cross sections" make different contributions to the unpolarized and spin-spin total cross sections, and must be weighted accordingly by the angular momentum coupling coefficients $F_q(Jlsl's')$. If we substitute $k = K = 0$ into Eq. (10), we find $F_q = \delta_{ll'}\delta_{ss'}$ for all values of q and J, and one obtains the familiar result that the unpolarized total cross section is simply a sum over the diagonal elements of the scattering matrix

$$\sigma_0 = \sum_{Jls} \sigma(Jlsls). \tag{17}$$

One of the consequences of working in the channel spin representation is that channel spin is a conserved quantity in the forward elastic scattering amplitude, and so $F_q = 0$ whenever $s' \neq s$. The spin-spin cross section, however, does include contributions from the off-diagonal S-matrix elements that mix orbital angular momenta l and $l \pm 2$. Expressed in terms of the partial-wave cross sections, the spin-spin cross section is

$$\sigma_{11} = \sum_{Jll's} \sigma(Jlsl's)\left\{ F_0(Jlsl's)\cos(\beta_A)\cos(\beta_a) + \frac{1}{2}\left[F_{-1}(Jlsl's) + F_1(Jlsl's)\right]\sin(\beta_A)\sin(\beta_a)\cos(\phi_A - \phi_a)\right\}, \tag{18}$$

where the explicit forms for $C_{1q}(\beta, \phi)$ in Eq. (10) have been substituted.

The longitudinal and transverse geometries correspond to $\beta_A = \beta_a = 0°$ and $\beta_A = \beta_a = 90°$, respectively, and so

$$\Delta\sigma_L = 2\sum_{Jll's} F_0(Jlsl's)\sigma(Jlsl's) \tag{19}$$

and

$$\Delta\sigma_T = 2\sum_{Jll's} F_1(Jlsl's)\sigma(Jlsl's), \tag{20}$$

since $F_{-1}(Jlsl's) = F_1(Jlsl's)$. Explicit values of F_0 and F_1 up to $l = 3$ are given in Table I.

TABLE I. The angular momentum coupling coefficients $F_0(Jlsl's)$ and $F_1(Jlsl's)$ of Eq. (10) up to $l = 3$. The subscripts 0 and 1 correspond respectively to the longitudinal and transverse spin geometries. The coupling coefficients for mixed orbital angular momentum states $l' = l \pm 2$ are listed at the bottom.

$^{(2s+1)}L_J$	$F_0(Jlsls)$	$F_1(Jlsls)$
$^1S_0$	-1	-1
$^3S_1$	$\frac{1}{3}$	$\frac{1}{3}$
$^1P_1$	-1	-1
$^3P_0$	-1	1
$^3P_1$	1	0
$^3P_2$	$\frac{1}{5}$	$\frac{2}{5}$
$^1D_2$	-1	-1
$^3D_1$	$-\frac{1}{3}$	$\frac{2}{3}$
$^3D_2$	1	0
$^3D_3$	$\frac{1}{7}$	$\frac{3}{7}$
$^1F_3$	-1	-1
$^3F_2$	$-\frac{1}{5}$	$\frac{3}{5}$
$^3F_3$	1	0
$^3F_4$	$\frac{1}{9}$	$\frac{1}{3}$
$^{(2s+1)}L_J - {}^{(2s+1)}L'_J$	$F_0(Jlsl's)$	$F_1(Jlsl's)$
$^3S_1 - {}^3D_1$	$\frac{2}{3}\sqrt{2}$	$-\frac{1}{3}\sqrt{2}$
$^3P_2 - {}^3F_2$	$\frac{2}{5}\sqrt{6}$	$-\frac{1}{5}\sqrt{6}$

To aid in the following discussion of n-^{3}He scattering, we write the explicit forms of σ_0, $\Delta\sigma_L$, and $\Delta\sigma_T$ in terms of partial-wave cross sections up to $l = 1$:

$$\begin{aligned}\sigma_0 = {} & \sigma(^1S_0) + \sigma(^3S_1) + \sigma(^1P_1) \\ & + \sigma(^3P_0) + \sigma(^3P_1) + \sigma(^3P_2),\end{aligned} \tag{21}$$

$$\begin{aligned}\Delta\sigma_L = {} & -2\sigma(^1S_0) + \frac{2}{3}\sigma(^3S_1) - 2\sigma(^1P_1) \\ & - 2\sigma(^3P_0) + 2\sigma(^3P_1) + \frac{2}{5}\sigma(^3P_2) \\ & + \frac{4}{3}\sqrt{2}\sigma(^3S_1 - {}^3D_1),\end{aligned} \tag{22}$$

and

$$\begin{aligned}\Delta\sigma_T = {} & -2\sigma(^1S_0) + \frac{2}{3}\sigma(^3S_1) - 2\sigma(^1P_1) \\ & + 2\sigma(^3P_0) + \frac{4}{5}\sigma(^3P_2) - \frac{2}{3}\sqrt{2}\sigma(^3S_1 - {}^3D_1).\end{aligned} \tag{23}$$

Here $\sigma(^{2s+1}L_J)$ refers to the $\sigma(Jlsls)$ partial-wave cross section defined in Eq. (16). Extension of these formulas to include higher partial waves follows from Table I. In the next section we shall discuss how this partial-wave decomposition may be used to extract information about the contributions of specific partial waves.

IV. CALCULATION OF $\Delta\sigma$ FOR n-^{3}He SCATTERING

The ^{4}He level scheme obtained from a comprehensive, charge-independent R-matrix analysis of n-^{3}He, p-^{3}H, and d-^{2}H scattering and reaction data [5] is shown

in Fig. 2. The isospin-1 parameters are taken from a Coulomb-corrected analysis of p-^{3}He data. This analysis finds evidence for a series of 15 excited states lying some 20–30 MeV above the ^{4}He ground state. They do not appear as sharp, well-isolated resonances in the n-^{3}He cross sections, but are instead broad, overlapping structures. Any theoretical description of the ^{4}He excited states must reproduce the positions and widths of these levels. Experimental determination of the states is hindered by the width of the levels and by the degree to which they overlap.

To investigate the sensitivity of the spin-spin cross section to the excited states of the α particle, we have calculated $\Delta\sigma_L$ and $\Delta\sigma_T$ for n-^{3}He data. The transmission of polarized neutrons through polarized ^{3}He has been measured previously [15,16]. Both experiments were performed using thermal neutrons and hence were only sensitive to S-wave scattering amplitudes. It is worth noting that the experiment of Paschell and Schermer [15] confirmed that 100% of the ^{3}He$(n,p)^3$H reaction proceeds through the $^1S_0$ partial wave at 0.11 eV. In this section we shall examine the sensitivity of polarized-neutron polarized ^{3}He to the P-wave amplitudes as well.

The S-matrix elements used in the calculations were obtained from four sources: (1) Hale's R-matrix analysis [5]; (2) the single-energy partial-wave analysis of Lisowski *et al.* [6] (Lisowski PWA); (3) the single-energy partial-wave analysis of Jany *et al.* [7] (Jany PWA); (4) a preliminary, multi-channel resonating group model (MCRGM) calculation of the ^{4}He continuum [8].

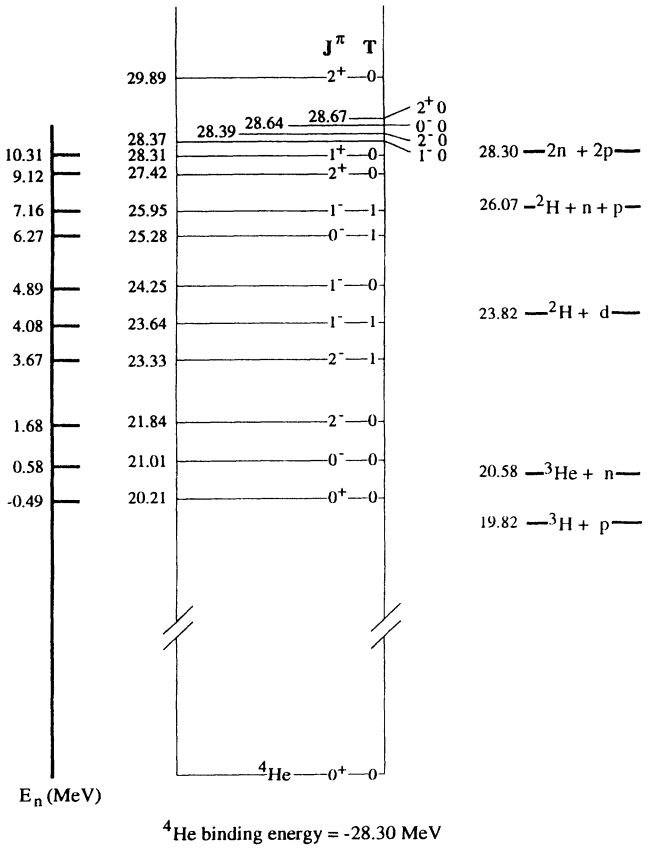

FIG. 2. The level scheme of ^{4}He as determined by the R-matrix analysis of Hale and co-workers [1,5]. The vertical bar on the left marks the position of the levels in the n-^{3}He laboratory frame, and the positions of the two-, three-, and four-body breakup thresholds are shown on the right.

The R-matrix analysis is a global parametrization of the $A = 4$ system. That is, the R-matrix parameters are varied to obtain simultaneous best fits to all $A = 4$ scattering and reaction data. In contrast, the two sets of partial-wave analyses are attempts to describe only the n-^{3}He two-body channel. The MCRGM matrix elements result from a microscopic, variational calculation that utilizes a Gaussian-parametrized version of the Bonn nucleon-nucleon potential [17]. We include two sets of partial-wave analyses (PWA's) because the PWA of Jany *et al.* is the most recent partial-wave analysis of n-^{3}He scattering in the few MeV energy region, but it does not cover as broad an energy range as that of Lisowski *et al.* Also, the Jany PWA used the R-matrix phase shifts as its starting parameters. One would therefore expect these latter two analyses to give similiar results. Table II compares many of the relevant parameters for the four sets of S-matrix elements.

The total (unpolarized) cross section is shown in Fig. 3. The R-matrix and phase-shift analyses describe the total cross section about equally well, whereas the MCRGM calculation does not quantitatively reproduce the experimental values above 1 MeV. As this is the region where $l = 1$ scattering begins to dominate, the inadequacy of the MCRGM calculations can probably be attributed to insufficient P-wave amplitudes. Comparing the individual matrix elements, we find the greatest discrepancy between the R-matrix and MCRGM results in the $^3P_2$ partial wave.

The R-matrix partial-wave contributions to the total cross section are shown in Fig. 4. According to the R-matrix analysis, partial waves corresponding to $l \geq 2$ contribute less than 4% of the total cross section between 0.1 and 10 MeV and thus are not shown in Fig. 4 [18]. The dominant partial waves below 100 keV are the two S waves, $^1S_0$ and $^3S_1$. Scattering through the $^3S_1$ partial wave is mostly elastic, whereas the large $^1S_0$ partial wave indicates the presence of the 0^+ resonance located 20.2 MeV above the ^{4}He ground state. This resonance

TABLE II. Parameters describing the S-matrix elements used in the n-^{3}He cross-section calculations. In the case of the R-matrix and MCRGM calculations, elements were obtained at laboratory energies separated by approximately 0.25 MeV below 1 MeV and by appoximately 2 MeV above 1 MeV. In these cases the phase shifts (both real and imaginary parts) varied smoothly and slowly, so that a cubic spline interpolation routine could be used to obtain phase shifts at intervals of approximately 0.1 MeV.

Analysis	Ref.	Energy range (MeV)	l_{max}	J_{max}
R matrix	[5]	0.1–10.0	3	4
MCRGM	[8]	0.14–12.14	2	3
Lisowski PWA	[6]	1.0–23.7	2	3
Jany PWA	[7]	1.0–3.7	2	3

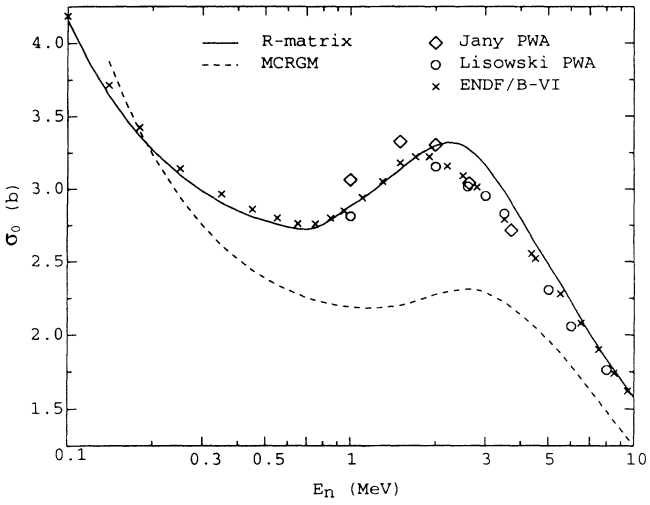

FIG. 3. The total (unpolarized) n-^{3}He cross section calculated using the four sets of S-matrix elements detailed in the text. The ENDF/B-VI [22] fit to the experimental values is also shown ($\times$'s).

is unstable against breakup into the p-^{3}H channel and is responsible for the enormous thermal neutron cross section of ^{3}He. The 0^+ resonance is customarily described as a breathing-mode oscillation.

The ^3P_J partial-wave cross sections are obviously related to the series of negative parity states in Fig. 2 between 21 and 25 MeV, beginning with a 0^- level at 21.0 MeV. De-Shalit and Walecka have pointed out that these low-energy states may be viewed as $(1s)^3(1p)$ excitations in a simple shell model of ^{4}He [19]. The spin of one of the nucleons is flipped, and it is elevated to the $(1p)$ orbital. The resulting nucleon-trinucleon cluster then has quantum numbers $l = 1$, $s = 1$, $J = 0$, 1, or 2, and isospin $T = 0$ or $T = 1$. These negative parity levels belong to the $\{15\}$ dimensional representation of SU(4) [20]. Another negative parity state with quantum numbers $s = 0$, $l = 1$, $J = 1$, and $T = 0$ belongs to the $\{15\}$ representation as well. Spin-dependent forces and charge-symmetry breaking are responsible for breaking the degeneracy of the $\{15\}$ supermultiplet.

We now describe how the spin-dependent total cross-section differences $\Delta\sigma_L$ and $\Delta\sigma_T$ reflect the excited structure of ^{4}He and how these observables may be used to delineate specific partial-wave information.

Calculated values of $\Delta\sigma_L$ and $\Delta\sigma_T$ using the four groups of matrix elements are shown in Fig. 5. At low energies (<500 keV) both $\Delta\sigma_L$ and $\Delta\sigma_T$ are large and negative, indicating that scattering primarily occurs between antiparallel spins. At these low energies the total cross section is dominated by the 0^+ resonance at 20.2 MeV in the ^{4}He system. A 0^+ resonance must have $F(Jlsl's) = -1$ for either the longitudinal or transverse geometry. Therefore the contribution of this state to the unpolarized cross section is doubled when the cross-section differences $\Delta\sigma_L$ and $\Delta\sigma_T$ are calculated [see Eqs. (22) and (23)]. As E_n increases, the ratio of triplet-to-singlet S-wave scattering increases, which along with

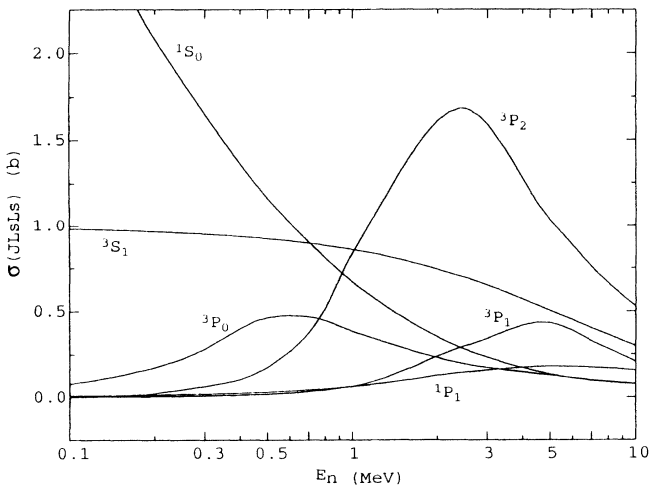

FIG. 4. The dominant R-matrix partial wave contributions to the n-^{3}He total cross section.

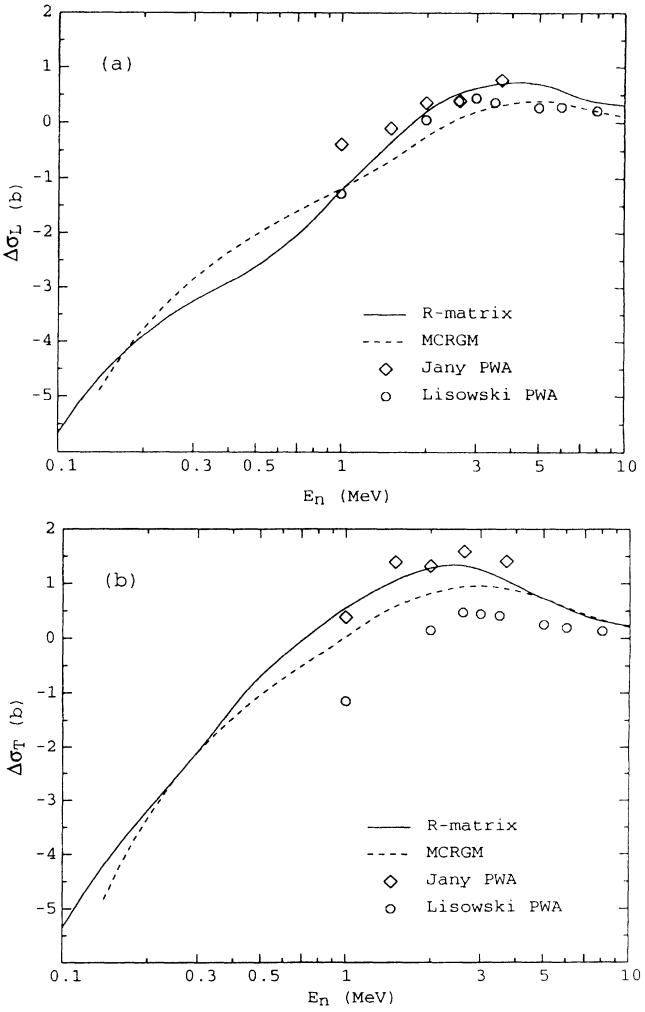

FIG. 5. Calculated values of (a) $\Delta\sigma_L$ and (b) $\Delta\sigma_T$ using the four set of S-matrix elements detailed in the text.

the emergence of P waves causes both $\Delta\sigma_L$ and $\Delta\sigma_T$ to cross through zero near 1 MeV.

Above 1 MeV, we see considerable disagreement in the various predictions of both $\Delta\sigma_L$ and $\Delta\sigma_T$. The main contributors in this energy region (according to the R matrix) are the $^3S_1$, $^3P_1$, and $^3P_2$ partial waves. However, the $^3P_1$ partial wave cannot contribute to $\Delta\sigma_T$ because $F_1(^3P_1) = 0$. Therefore $\Delta\sigma_T$ is mainly a measure of the $^3P_2$ strength in this energy region, with some contribution from the $^3S_0$ and $^1P_1$ partial waves. Correspondingly, between 1 and 5 MeV (where the $^3P_2$ wave is at a maximum) the calculated values of $\Delta\sigma_T$ disagree by as much as 1.5 barns. This would indicate that there is no consensus as to the strength of the $^3P_2$ partial wave. Comparing the individual matrix elements, we find similarity between the $^3P_2$ waves of the Lisowski PWA and the MCRGM calculation, but the R-matrix and Jany $^3P_2$ waves are considerably stronger. This explains why the latter two analyses predict higher values of $\Delta\sigma_T$ as well, since the $^3P_2$ wave makes a positive contribution to $\Delta\sigma_T$ (see Table I). The Lisowski (PWA) prediction of $\Delta\sigma_T$ is noticably lower than the other three predictions. The difference is the unusually strong $^1D_2$ partial wave of Lisowski [18], which lowers $\Delta\sigma_T$ by as much as one barn.

The sensitivity to the $^3P_2$ wave is reduced by half in the longitudinal geometry (see Table I), and therefore, slightly better agreement is observed in the values of $\Delta\sigma_L$, particularly above 2 MeV. The effect of the $^3P_2$ partial wave may be removed entirely using the linear combination $(3\,\Delta\sigma_L - \Delta\sigma_T)$. At the same time, this linear combination magnifies the $^3P_1$ contribution by a factor of 6.

The difference $(\Delta\sigma_T - \Delta\sigma_L)$ for the four sets of calculations is shown in Fig. 6. All S-wave and spin-singlet contributions to the total cross section are removed by this linear combination of $\Delta\sigma_L$ and $\Delta\sigma_T$ [21]. Therefore, this combination is extremely sensitive to the low-lying negative-parity states shown in Fig. 2. The large difference around 700 keV is a result of $^3P_0$ scattering (a 0^- resonance at 21.0 MeV). For the $^3P_0$ partial wave, scattering only occurs between *antiparallel* spins in the longitudinal spin geometry ($F_0 = -1$), whereas the opposite is true for the transverse geometry ($F_1 = +1$). Therefore, the contribution of the $^3P_0$ partial wave is magnified by a factor of 4 when the difference $(\Delta\sigma_T - \Delta\sigma_L)$ is taken. Combinations utilizing the unpolarized cross section σ_0 can be made to exploit other partial waves as well. In particular, we find that below about 1 MeV,

$$\Delta\sigma_T - \Delta\sigma_L \simeq 4\,\sigma(^3P_0), \tag{24}$$

$$2\,\sigma_0 + \Delta\sigma_L \simeq \frac{10}{3}\,\sigma(^3S_1), \tag{25}$$

$$\Delta\sigma_L + \Delta\sigma_T \simeq 4\,\sigma(^1S_0) + \frac{4}{3}\,\sigma(^3S_1). \tag{26}$$

To illustrate this point, we have included the R-matrix $^3P_0$ partial wave in Fig. 6 (dash-dotted line). It is evident that the scattering amplitudes for these lowest partial waves can be completely and uniquely extracted from a complete measurement of $\Delta\sigma_L$ and $\Delta\sigma_T$ below 1 MeV.

Finally, we see in Fig. 6 that there is essentially no difference between the calculated values of $\Delta\sigma_L$ and $\Delta\sigma_T$ when the phase shifts of Lisowski *et al.* are used. Referring again to Table I, we find this indicative of strong S-wave and spin-singlet scattering amplitudes. Examination of the individual partial waves agrees with this conclusion. The $^3S_1$ and $^1D_2$ partial waves are considerably stronger in the Lisowski PWA than in any of the other three analyses.

The sensitivity of $\Delta\sigma_L$ and $\Delta\sigma_T$ to the $l \geq 2$ scattering as well as the amplitudes corresponding to mixed orbital angular momentum can be determined from Table I. However, in the energy range under consideration, such contributions to the total cross section are relatively unimportant in comparison to the S- and P-wave amplitudes (an exception is Lisowski's $^1D_2$ partial wave [18]). Linear combinations of σ_0, $\Delta\sigma_L$, and $\Delta\sigma_T$ can be made to emphasize these partial waves at higher energies once the effects of $l = 0$ and $l = 1$ scattering have been well determined.

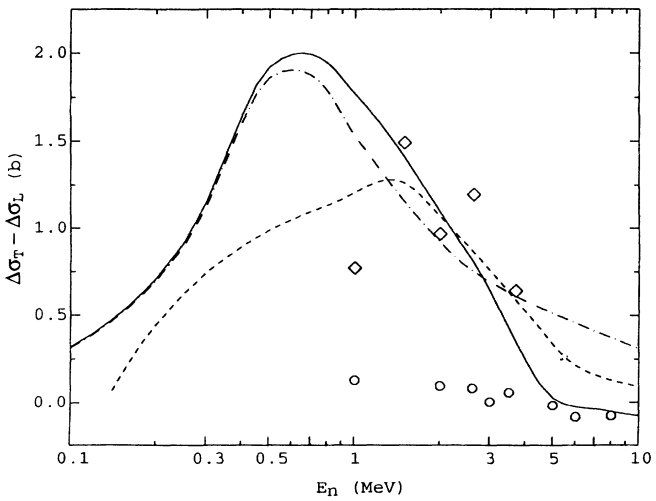

FIG. 6. Calculated values of the quantity $(\Delta\sigma_T - \Delta\sigma_L)$ using the four sets of S-matrix elements detailed in the text. Symbols same as Fig. 5. Also shown (dash-dotted line) is 4 times the $^3P_0$ cross section from Fig. 4, $4\sigma(^3P_0)$.

V. SUMMARY AND CONCLUSIONS

The formalism for the spin-dependent total cross-section difference $\Delta\sigma$ has been derived. For the particular case of spin-1/2–spin-1/2 scattering, a partial-wave decomposition has been performed. Using four independent analyses of n-^{3}He scattering, the polarization observables $\Delta\sigma_L$ and $\Delta\sigma_T$ have been calculated. The results reflect much of the resonant structure of ^{4}He. Comparison between the four sets of calculations indicates qualitatively good agreement. However, differences exist that in most cases can be traced to one particular scattering amplitude.

With a complete measurement of σ_0, $\Delta\sigma_L$, and $\Delta\sigma_T$ below about 500 keV, one can in principle uniquely determine the partial-wave amplitudes for $^1S_0$, $^3S_1$, and $^3P_0$

scattering. The situation at higher energies is complicated by the presence of additional partial waves. However, linear combinations of σ_0, $\Delta\sigma_L$, and $\Delta\sigma_T$ may be used to enhance the sensitivity to one particular partial wave while diminishing the effect of another. In this manner the spin-dependent total cross section can determine specific partial-wave scattering amplitudes, and in turn, information about the ^{4}He scattering states.

ACKNOWLEDGMENTS

The authors acknowledge Professor D. R. Lehman and Professor A. C. Fonseca for many valuable discussions on the few-body scattering problem. This work was supported in part by the U.S. Department of Energy, Office of High Energy and Nuclear Physics, under Contracts Nos. DE-FG05-88-ER40441 and DE-FG05-91-ER40619.

[1] D. R. Tilley, H. R. Weller, and G. M. Hale, Nucl. Phys. **A541**, 1 (1992); this compilation article contains a complete reference guide to experimental and theoretical work on $A = 4$ nuclei since 1973.

[2] H. Kamada and W. Glöckle, Nucl. Phys. **A548**, 205 (1992).

[3] N. W. Schellingerhout, J. J. Schut, and L. P. Kok, Phys. Rev. C **46**, 1192 (1992).

[4] W. Glöckle and H. Kamada (private communication).

[5] G. M. Hale, D. C. Dodder, and K. Witte (unpublished).

[6] P. W. Lisowski, R. L. Walter, C. E. Busch, and T. B. Clegg, Nucl. Phys. **A264**, 188 (1976).

[7] P. Jany *et al.*, Nucl. Phys. **A483**, 269 (1988).

[8] H. M. Hofmann (unpublished).

[9] C. R. Gould *et al.*, Int. J. Mod. Phys. A **5**, 2181 (1990).

[10] V. P. Alfimenkov, V. N. Efimov, T. T. Panteleev, and Y. I. Fenin, Yad. Fiz. **17**, 293 (1973) [Sov. J. Nucl. Phys. **17**, 149 (1973)].

[11] G. R. Satchler *et al.*, in *Proceedings of the 3rd International Symposium on Polarization Phenomena in Nuclear Reactions, 1970*, edited by H. H. Barschall and W. Haeberli (The University of Wisconsin Press, Madison, 1971), pp. xxv–xxix.

[12] D. M. Brink and G. R. Satchler, *Angular Momentum* (Oxford University Press, New York, 1971).

[13] G. R. Satchler, *Direct Nuclear Reactions* (Oxford University Press, New York, 1983).

[14] R. J. N. Phillips, Nucl. Phys. **43**, 413 (1963).

[15] L. Passell and R. I. Schermer, Phys. Rev. **150**, 146 (1966).

[16] A. Benoit *et al.*, Can. J. Phys. **65**, 57 (1987).

[17] H. Kellermann, H. M. Hofmann, and C. Elster, Few-Body Syst. **7**, 31 (1989).

[18] The partial-wave analysis of Lisowski is unusual in that it predicts a very strong $^1D_2$ contribution to the total cross section. This partial-wave cross section is a maximum of 0.5 barns at 1 MeV.

[19] A. De-Shalit and J. Walecka, Phys. Rev. **147**, 763 (1966).

[20] L. L. Foldy and J. D. Walecka, Nuovo Cimento **34**, 1026 (1964).

[21] The $\Delta\sigma_T - \Delta\sigma_L$ combination is sensitive to $l = 0$ scattering in that off-diagonal elements of the S matrix corresponding to $^3S_1$-$^3D_1$ transitions do not disappear in this particular combination of $\Delta\sigma_L$ and $\Delta\sigma_T$ (see Table I). Below $E_n \approx 1$ MeV their contribution to the spin-spin cross section is negligible.

[22] G. Hale, D. Dodder, and P. Young, "ENDF/B-VI Data File for ^{3}He," National Nuclear Data Center, Brookhaven National Laboratory, Upton, New York, 1991 (unpublished).